Department of AERONAUTICS and ASTRONAUTICS
STANFORD UNIVERSITY

EFFECT OF NOSE SHAPE AND MASS OF THE IMPACTOR ON IMPACT DAMAGE OF LAMINATED COMPOSITES

FINAL REPORT

FU-KUO CHANG

NOVEMBER 21, 1994

U.S. ARMY RESEARCH OFFICE

DAAL03-91-G-0087

STANFORD UNIVERSITY

MASTER COPY KEEP THIS COPY FOR REPRODUCTION PURPOSES

REPORT DOCUMENTATION PAGE

Form Approved
OMB No. 0704-0188

1. AGENCY USE ONLY (Leave blank)	2. REPORT DATE	3. REPORT TYPE AND DATES COVERED
	11/21/94	Final Report 3/15/91 - 3/14/94

4. TITLE AND SUBTITLE
Effect of Nose Shape and Mass of the Impactor on Impact Damage of Laminated Composites

5. FUNDING NUMBERS
DAAL03-91-G-0087

6. AUTHOR(S)
Fu-Kuo Chang

7. PERFORMING ORGANIZATION NAME(S) AND ADDRESS(ES)
Department of Aeronautics and Astronautics
Stanford University
Stanford, CA 94305-4035

8. PERFORMING ORGANIZATION REPORT NUMBER

9. SPONSORING / MONITORING AGENCY NAME(S) AND ADDRESS(ES)
U. S. Army Research Office
P. O. Box 12211
Research Triangle Park, NC 27709-2211

10. SPONSORING / MONITORING AGENCY REPORT NUMBER
ARO 28253.1-EG

11. SUPPLEMENTARY NOTES
The view, opinions and/or findings contained in this report are those of the author(s) and should not be construed as an official Department of the Army position, policy, or decision, unless so designated by other documentation.

12a. DISTRIBUTION / AVAILABILITY STATEMENT
Approved for public release; distribution unlimited.

12b. DISTRIBUTION CODE

13. ABSTRACT *(Maximum 200 words)*

The investigation studied impact damage resistance of laminated composites caused by a low-velocity foreign object. Effects of material interfacial strength and impactor's mass and nose size on damage resistance were the study's concern. An analytical model was developed for predicting the dynamic response of composites during impact. The model consists of damage accumulation prediction and material degradation modeling. Damage accumulation criteria were adopted for predicting failure and mode of failure due to impact. Appropriate material constitutive relations were also proposed to relate strains to stresses for material that was inflicted with impact damage. The Hertzian contact law was modified by taking into account material degradation during impact. The proposed model and modified Hertzian contact law were implemented in a transient dynamic finite element analysis designated "3DIMPACT." The code predicts force response and damage accumulation of a composite during impact. Composites with and without toughening interleaves were tested experimentally to verify the model and the computer code. The effect of the impactor's size and nose radius was considered in verifying the code, very useful for evaluating impact resistance and for screening materials.

14. SUBJECT TERMS	15. NUMBER OF PAGES
	38
	16. PRICE CODE

17. SECURITY CLASSIFICATION OF REPORT	18. SECURITY CLASSIFICATION OF THIS PAGE	19. SECURITY CLASSIFICATION OF ABSTRACT	20. LIMITATION OF ABSTRACT
UNCLASSIFIED	UNCLASSIFIED	UNCLASSIFIED	UL

TABLE OF CONTENTS

ABSTRACT

An investigation was performed to study the impact damage resistance of laminated composites caused by a low-velocity foreign object. The effects of material interfacial strength and impactor's mass and nose size on the damage resistance were the major concern of the study. An analytical model was developed for predicting the dynamic response of composites during impact. The model consists of damage accumulation prediction and material degradation modeling. Damage accumulation criteria were adopted for predicting failure and the mode of failure due to impact. Appropriate material constitutive relations were also proposed to relate strains to stresses for the material that was inflicted with impact damage. The Hertzian contact law was also modified by taking into account material degradation during impact.

The proposed model and the modified Hertzian contact law were implemented in a transient dynamic finite element analysis, designated as "3DIMPACT." The code can predict the force response and damage accumulation of a composite during impact. Composites with and without toughening interleaves were tested experimentally to verify the model and the computer code. The effect of the impactor's size and nose radius was also considered in verifying the code. Overall, the prediction agreed very well with the test data. The code could be very useful for evaluating the impact resistance of a composite and also for screening materials.

I. INTRODUCTION

One of the major concerns in the design of composite structures is impact damage. Organic matrix fiber-reinforced laminated composites are very susceptible to transverse impact, especially at low velocities. Low-velocity impact can cause damage, including matrix cracks, delaminations, and fiber breakage, which is embedded inside the composites. Such damage is very difficult to detect with the naked eye and can cause significant reductions in the strength and stiffness of the materials.

Hence, the knowledge of damage resistance of composites is critically important for their application. It has been observed [1-5] that the impact damage strongly depended upon many factors such as material properties of composites, laminate ply orientation and thickness, as well as the mass and the shape of the projectile. Interleaved composites or composites with toughened interfaces have been shown experimentally to produce higher damage resistance to impact [6,7]. Therefore, it is possible to improve the impact resistance of a laminated composite by properly designing the material and the structures.

Numerous investigations have been conducted on this subject, including experimental and analytical work. Because of the overwhelming amount of literature related to the subject, only some of the studies are selectively cited here [1-43]. Because the damage was mostly embedded inside the materials, tested specimens were usually C-scanned or X-rayed, and then sliced in pieces to inspect the damage.

Several analytical models [23-43] have been developed to study the transient dynamic response of composites due to impact. However, the major attention of most of the analytical studies was focused either on the contact force of an impactor or on the response of the plates without consideration of impact damage. A recent study by the P.I. and his associates [42,43] has resulted in a semi-empirical model as well as a computer code,"3DIMPACT," based on the observed impact damage mechanisms for estimating the extent of impact damage in laminated composites. No material degradation due to impact was considered in the model. By appropriately selecting an empirical parameter, the code was shown to produce a good correlation with the test data.

Since impact can result in significant damage, which can degrade material properties and alter the impact response of the composites, it is believed that in order to accurately evaluate the impact resistance of composites, the effect of damage must be considered in the analysis. Therefore, the objective of this study was to enhance the ability of the previous model by taking into account the effect of damage accumulation on the material and on the response of the structure during impact. The model would be then implemented in the computer code "3DIMPACT" so as to be able to assess the impact resistance of composites as a function of material properties and design parameters.

This report summarizes the results of the study. Both the model and the experiments will be described briefly and the comparisons between the predictions and the data will also be selectively presented. A detailed description of the study and the results was documented in Reference 44 as a Ph.D. dissertation.

II. PROBLEM STATEMENT

Consider a fiber-reinforced laminated composite panel with and without toughening interleaves, and subjected to transverse impact by a low-velocity spherical-nose impactor as shown in Figure 1. The ply orientation of the laminate can be arbitrary but must be symmetric with respect to its middle plane. The impactor's radius and mass may vary. For a given mass and nose radius of the impactor, the following are to be determined:

(1) The velocity of the impactor required to initiate the impact damage.

(2) The force-time history of the impact.

(3) The extent of damage and failure modes inside the laminate.

(4) The residual stiffness of the composite after impact.

III. THE MODEL

The model consists of damage accumulation prediction and material degradation

modeling. Failure criteria were adopted for predicting the type and the extent of the damage in composites due to impact, and appropriate material constitutive relations were proposed to estimate the residual properties of damaged composites due to impact.

3.1 DAMAGE ACCUMULATION PREDICTION

Low-velocity impact damage may consist of matrix cracks, delaminations, and fiber breakage. It has been shown [2,3] that matrix cracking is the initial damage mode. Matrix cracks can induce delaminations immediately along the bottom or upper interface of the cracked layer, depending on the position of the layer in the laminate. Fiber breakage may also occur inside and on the surface of the laminate.

Therefore, in order to predict the impact damage, a model must be capable of predicting these three failure modes in a correct sequence. Accordingly, three failure criteria were adopted for predicting matrix cracking, impact-induced delamination, and fiber breakage.

Matrix Cracking Criterion

In order to predict the occurrence of the critical matrix cracks, the matrix failure criterion proposed previously by the authors [42,45] will be adopted here; the criterion can be expressed as

$$\left(\frac{\overline{\sigma}^{*}_{yy}}{Y}\right)^2 + \left(\frac{\overline{\sigma}_{xy}}{S}\right)^2 = e_M^2 \qquad \begin{cases} e_M \geq 1 & \text{Failure} \\ e_M < 1 & \text{No failure} \end{cases} \qquad \begin{cases} Y = Y_t & \text{if } \overline{\sigma}_{yy} \geq 0 \\ Y = Y_c & \text{if } \overline{\sigma}_{yy} < 0 \end{cases} \tag{1}$$

where the subscript of x and y are the local coordinates of the nth layer parallel and normal to the fiber directions, respectively, and z is the out-of-plane direction. $\bar{\sigma}^{*}_{yy}$ is the effective principal stress in the ply and is defined as follows:

$$\bar{\sigma}^{*}_{yy} = \frac{\bar{\sigma_{yy}}}{2} + [(\frac{\bar{\sigma}_{yy}}{2})^2 + \bar{\sigma}^2_{yz}]^{\frac{1}{2}} \tag{2}$$

Y_t and Y_c are the intraply transverse tensile and compressive strengths, respectively [45], and S is the intraply shear strength. Both Y_t and S strongly depend upon the thickness of the ply group and the ply orientations of the immediate neighboring plies. Y_t and S are the stresses corresponding to the first matrix cracking and can be determined based on the theory of elasticity and the principle of the conservation of energy. Details of the derivation are given in Ref. [44].

Whenever the calculated effective stresses in any one of the plies in the laminate first satisfy the criterion ($e_M = 1$) during impact, initial impact damage is predicted. It was assumed then that the matrix crack would propagate throughout the thickness of the ply group which contains the cracked ply. The time t corresponding to the initial damage is designated as t_M. A delamination could immediately follow from the location of the matrix crack along the interfaces of the ply group. As the time increases ($t > t_M$) during impact, additional matrix cracking could be produced in the other layers. Hence, the criterion should continuously be applied to the other layers for determining any additional matrix failure. If no additional matrix cracking is found at any other layer during impact, then the impactor's velocity associated with the first matrix cracking is referred to as the impact velocity threshold, which is the velocity required to just cause the initial impact damage of the laminate.

Impact-Induced Delamination Criterion

It was believed that delamination growth due to low-velocity impact would occur only when the following two sequential conditions were met:

(1) one of the ply groups immediately above or below the concerned interface has failed due to matrix cracking and

(2) the combined stresses governing the delamination growth mechanisms through the thicknesses of the upper and lower ply groups of the interface reach a critical value.

Based on the above second statement, the following impact-induced delamination criterion originally proposed by Choi and Chang [42] was adopted and modified as follows:

$$\left[\left(\frac{\overline{\sigma}_{yz}}{S_{yz}}\right)^2+\left(\frac{\overline{\sigma}_{xz}}{S_{xz}}\right)^2+\left(\frac{\overline{\sigma}_{yy}}{Y}\right)^2\right]=e_D^2 \tag{3}$$

where $\overline{{}^{n}\sigma}_{yz}$ and ${}^{n+1}\overline{\sigma}_{xz}$ are the interfacial shear stresses on the surfaces above and below the ply under consideration, respectively. S_{yz} and S_{xz} are the interlaminar shear strengths in the direction perpendicular or parallel to the fiber direction of the ply under consideration, respectively. Similar to Y_t and S, the values of S_{yz} and S_{xz} may also depend upon the ply orientation of the neighboring plies. Determination of these distributions as a function of the ply orientation will be discussed in Section IV.

Note that it was found that the empirical parameter D_a originally proposed for Eq. (3) was not necessary once the interlaminar strength distributions were determined from experiments.

Fiber Breakage Criterion

Fiber breakage in the laminate was predicted by the following criterion:

$$\left(\frac{\overline{\sigma}_{xx}}{X_t}\right)^2=e_f^2 \tag{4}$$

where X_t is the longitudinal tensile strength of the unidirectional composite.

Based on the previous studies [2,3,42], the matrix cracking criterion should be applied first to predict matrix failure. Once a critical matrix crack is predicted in a layer, the delamination criteron and the fiber breakage criterion will then be applied to estimate the extent of the delamination and the fiber breakage areas, respectively. The local damage may cause material degradation in the damaged ply and affects the subsequent dynamic response of the composite. Therefore, appropriate material

constitutive relations are needed to assess the residual properties of the composite containing impact damage. The relationships between the mechanical properties of the composite and the type and extent of the damage will be established in the next section.

3.2 MATERIAL DEGRADATION MODELING

Matrix Cracking

Matrix crack density has been utilized widely as a means for characterizing the residual properties of composites containing matrix crack damage. The constitutive relations of the m-th ply in a laminate as a function of crack density ϕ have been developed recently by Shahid and the P.I. [45] and can be expressed on the material axes as follows:

$$[Q(\phi)]_m = \begin{pmatrix} Q_{xx}(\phi) & Q_{xy}(\phi) & 0 \\ Q_{yx}(\phi) & Q_{yy}(\phi) & 0 \\ 0 & 0 & Q_{ss}(\phi) \end{pmatrix}_m \tag{5}$$

where $Q_{ij}(\phi)$ $(i,j = x,y,z)$ are the components of the effective residual stiffness of a ply at a given crack density ϕ.

Eq. (5) may vary from layer to layer, depending upon the ply orientation of the laminate. It was assumed in Eq. (5) that the out-of-plane engineering constants, E_{zz}, G_{xz}, G_{yzz}, ν_{xz}, and ν_{yz}, were unaffected by matrix cracking.

The crack density in Eq. (5) would increase if the stresses continue to increase. Because matrix cracks accumulate rapidly during impact, it was assumed that once the matrix cracking criterion is predicted, cracks would immediately reach the saturation density, ϕ_o, within the area where the stresses satisfy the criterion. Accordingly, the effective engineering properties of each degraded ply can be expressed in terms of $Q_{ij}(\phi_o)$ of the effective ply stiffness as follows:

$$E_{xx}^D = \frac{Q_{xx}(\phi_o)}{m} \tag{6.1}$$

$$E_{yy}^D = \frac{Q_{yy}(\phi_o)}{m} \tag{6.2}$$

$$\nu_{xy}^D = \frac{Q_{xy}(\phi_o)}{Q_{yy}(\phi_o)} \tag{6.2}$$

$$\nu_{yx}^D = \frac{Q_{xy}(\phi_o)}{Q_{xx}(\phi_o)} \tag{6.3}$$

$$G_{xy}^D = Q_{ss}(\phi_o) \tag{6.4}$$

where $m = [1 - \frac{Q_{xy}^2}{Q_{xx}Q_{yy}}]^{-1}$, and the superscript D denotes degraded properties.

Impact-Induced Delamination

If delamination failure is predicted after matrix cracking has occurred, cracks would be generated along the interfaces of the cracked ply, resulting primarily in reduction of out-of-plane stiffness of the laminate. Since the delamination is induced by intraply matrix cracks, the effect of the delamination on the laminate stiffness can be taken into account by appropriately reducing the out-of-plane stiffness of the cracked ply.

Once a ply has suffered both interply and intraply cracks, the actual effective stiffness of the cracked ply in the composite is very difficult to be determined analytically or experimentally. Since the cracks have saturated in the ply, it was assumed in the proposed model that such a cracked ply in the damaged area can be treated as a transversely isotropic medium. As a result, the out-of-plane engineering properties of the cracked ply could have the following simple expressions:

$$E_{xx}^D = \frac{Q_{xx}(\phi_o)}{m} \tag{7.1}$$

$$E_{yy}^D = \frac{Q_{yy}(\phi_o)}{m} \tag{7.2}$$

$$\nu_{xy}^D = \frac{Q_{xy}(\phi_o)}{Q_{yy}(\phi_o)} \tag{7.3}$$

$$\nu_{yx}^D = \frac{Q_{xy}(\phi_o)}{Q_{xx}(\phi_o)} \tag{7.4}$$

$$G_{xy}^D = Q_{ss}(\phi_o) \tag{7.5}$$

$$E_{zz}^D = E_{yy}^D \tag{7.6}$$

$$G_{xz}^D = G_{xy}^D \tag{7.7}$$

$$\nu_{xz}^D = \nu_{xy}^D \tag{7.8}$$

$$\nu_{zx}^D = \nu_{xy}^D \tag{7.9}$$

$$\nu_{yz} = \nu_{zy} \tag{7.10}$$

where no degradation was assumed for ν_{yz} for preserving the assumption of transverse isotropy.

Fiber Breakage

If the fiber breakage criterion is predicted, the amount of the material degradation depends upon the size of the area where the stresses satisfy the fiber failure criterion. Based on the concept of continuum mechanics, a degradation parameter d_f will be multipled with all the engineering properties [45], where d_f can be expressed as

$$d_s = e^{(\frac{A_f}{\delta^2})^\beta} \tag{8}$$

where A_f is the area where the stresses satisfy the fiber breakage criterion, and δ is the fiber interaction length which can be estimated from the micromechanics [45]. β is the rate of the material degradation due to fiber breakage. Any value greater than 8 was appropriate for graphite/epoxy composites.

It is worth noting that the sequence in applying the failure criteria and material constitutive relations is very important for accurately predicting impact damage. Matrix cracks should be evaluated first. If matrix cracking is predicted, the impact-induced delamination and fiber breakage criteria should then be applied to estimate the extent of the delamination and fiber breakage areas. The procedure has to be

repeated at the other layers during impact. The final size of each delamination is determined by the area within which the stress components satisfy the delamination failure criterion during the entire duration of impact.

IV. THE HERTZIAN CONTACT LAW

The Hertzian contact law has been widely utilized to model the force response of an impactor during impact. The force-indentation relationship for low-velocity impact (no penetration) is normally generated by a static indentation test. The result of the test data was then fitted to the contact law in order to select a power constant for a particular target material. However, experiments have shown that the force-indentation relationship upon loading is different from unloading. In general, upon loading, the Hertzian contact law can be expressed [42,46] as

$$F = \kappa \alpha^{\gamma} \tag{9}$$

Thus, the contact force F can be related to the indentation depth α (the distance between the center of the projectile's nose and the mid-surface of the plate). κ is the contact stiffness, and γ is the power constant which has to be determined from the static identation test.

The contact stiffness κ is given as

$$\kappa = \frac{4}{3}\sqrt{r}\ \frac{1}{[k_s + k_t]} \tag{10}$$

where r is the radius of the impactor. k_t can be related to the properties of the target, while k_s is related to projectile properties and is given as

$$k_s = \frac{(1 - \nu_s^2)}{E_s} \tag{11}$$

where ν_s and E_s are the Poisson's ratio and the Young's modulus of the impactor,

respectively.

For laminated composites, k_t can be expressed directly in terms of laminate properties [47, 48]. However, once damage occurs in the laminate, both k_t and γ may not remain as constants, especially for k_t, which may be a function of the type and the extent of the damage in the target.

Accordingly, in this study, the value of k_t was recalculated at every time step based on the degraded material properties. The detailed derivation and implementation of the k_t in the analysis is described in Reference 44.

Upon unloading, the predicted contact force based on the contact law in Eq. (9) deviates from the measured contact force for a given indentation. It has been shown [49] that the contact law in Eq. (9) produces a longer impact duration upon unloading. Based on the test data, an empirical expression was suggested by Sun et al [32,33] for the force-identation relation. However, such an empirical expression could not be generalized and is difficult to apply once damage starts to accumulate in the target.

Therefore, in the study, the contact law in Eq. (9) was modified to take into account local damage, but was still used for both loading and unloading cases. Accordingly, it is expected that using the modified contact law, the dynamic force response upon unloading may not be accurate. This may affect the accuracy of the stresses and deformations of the target upon unloading. However, it will be demonstrated that most impact damage is induced upon loading. Since the post-impact dynamic response is out of the scope of the interest, this approach was adequate for the present study.

V. THE FINITE ELEMENT ANALYSIS

The "3DIMPACT" computer code, previously developed by Choi and Chang [42], was modified by implementing the proposed model. The finite element analysis was needed for calculating the stresses and strains inside the composites during impact.

The information regarding finite element procedures was given extensively in [35,42]. Here, only a brief description of the analytical approach will be given as follows:

The analysis was based on a three-dimensional linear elasticity theory. The materials in each layer were considered homogeneous and orthotropic. Accordingly, the equilibrium equations at instant time t in a variational form can be expressed as [42]

$$0 = \int_{\Omega} w_i \rho u_{i,tt} dv + \int_{\Omega} e_{ij} E_{ijkl} \epsilon_{kl} dv - \int_{\Gamma} w_i \sigma_{ij} n_j dA \tag{12}$$

where σ_{ij} are the stresses, ϵ_{kl} are the strains, ρ is the density, $u_{i,tt}$ are the accelerations ($u_{i,tt} = \partial^2 u_i / \partial t^2$), w_i are the arbitrary variational displacements, e_{ij} are the strains from the arbitrary variational displacements, Ω is the entire plate volume, Γ is the surface of the plate, n_j is the outward unit normal vector on the plate surface, and E_{ijkl} are the material properties of the laminate, which vary from layer to layer according to the ply orientation of the composite.

It has been shown that thermal residual stresses could reduce the impact resistance of composites [2,3]. The thermal stresses due to fabrication were calculated based on the theory of linear elasticity. The thermal stresses were combined with the mechanical stresses calculated from Eq. (12) to determine the damage state in the failure criteria.

In order to solve Eq.(1), the distribution of the contact force, $F(= \sigma_{ij} n_j)$, between the impactor and the impacted laminate must first be known. The Hertzian contact law was utilized to generate the contact force. However, the contact stiffness was adjusted according to the amount of damage inside the target.

An eight-node brick element incorporating incompatible modes developed previously by Wu and Chang [35] was used in the finite element calculations. The inclusion of incompatible modes was to improve the accuracy in calculating the bending stiffnesses and the interlaminar shear stresses. A direct Gauss quadrature integration scheme was adopted [39] through the element thickness to account for the change in material properties from layer to layer within the element. Therefore, plies with

different ply orientations could be grouped in an element, resulting in a significant reduction in computational time and memory space for the 3-dimensional analysis.

The contact area may increase upon loading and decrease upon unloading during the impact. The contact force was assumed to be distributed in a normal distribution over the area [44].

IV. EXPERIMENTS

4.1 INTERLAMINAR SHEAR STRENGTHS

Experiments were conducted to measure the interlaminar shear strengths, S_{xz} and S_{yz}, as a function of the ply orientation mismatch. Information about these interlaminar shear strengths is required from the impact-induced delamination criterion. The shear strengths S_{xz} and S_{yz} of a ply in a laminate are defined as the interfacial shear strengths along the fiber direction or normal to the fiber direction of the ply under consideration, respectively. Accordingly, depending upon the ply orientation, the interlaminar shear strengths may vary with the ply orientation mismatch.

The short beam shear test was selected for measuring the interlaminar shear strength. In order to evaluate the effect of ply angle mismatch on the shear strengths, the ply orientations of the specimens were carefully selected for the tests.

The interlaminar shear strength was taken as the stress at the interface corresponding to the collapse load of the specimens. In order to calculate shear stresses on the interfaces, the classical lamination theory was adopted to calculate the inplane stresses based on the three-point bending solutions. The out-of-plane shear stresses were then determined by employing the three-dimensional equilibrium equations with appropriate boundary conditions.

A summary of the interlaminar shear strength distributions between two neighboring plies as a function of the mismatch of the ply angles is shown in Figures 2 and 3. Apparently, the difference in ply angles affects significantly the interlaminar shear

strength. Additionally, because the distributions of S_{yz} and S_{xz} are considerably different, it is expected that the growth of interfacial delamination can be different in the direction parallel and normal to the fiber direction of the ply under consideration.

4.2 COMPOSITES WITH AND WITHOUT INTERLEAVES

In order to verify the proposed model, composites with and without toughening interleaves were fabricated. T300/976 composites and FM300 thermoset interleaves were selected for the study. The thickness of a single interleaf is about one fourth of the composite prepreg thickness. Numerous ply orientations were chosen. The dimensions of each specimen were 10 cm long and 7.6 cm wide.

All the specimens were cured without thermal-induced pre-matrix cracks. All the specimens were cut by a diamond-coated saw and X-rayed after the cutting to inspect any internal damage due to manufacturing and cutting. No apparent damage was found from the X-radiographs after cutting all the specimens.

Figure 4 shows schematically the impact test facility used for the study. A spherical-nosed impactor was selected for the study. The radius of the spherical nose head made of steel was 0.635 cm. The specimens were firmly clamped along two parallel edges as shown in Figure 4.

The results of the X-radiograph examinations of all the tested specimens showed consistently that the laminates with interleaves sustained higher energy impact at the same damage size. The selected results of the comparison are shown in Figures 5-7. It is noted that the double slashes "//" appearing in the ply orientations of these figures represented an interleaf at the location. The damage area in the figures was estimated directly from the X-radiographs. Apparently, both impact velocity threshold and impact damage size were sensitive to the presence of the interleaves.

V. COMPARISON AND VERIFICATION

5.1 EFFECT OF DAMAGE ON FORCE RESPONSE

Test data available in the literature were selected and utilized to verify the model and the computer code. First, the predictions were compared with the data generated from heavy mass/low velocity impact. Secondly, the effect of the impactor's mass on the impact response was evaluated for a given impact energy.

Heavy Mass-Low Velocity Impact

Figures 8-10 compared the force-time history of a heavy impactor on IM7/954-2 composites between the predictions and the measurements. The test data were obtained from Lockheed [51]. Numerical simulations of the test condition were performed with and without the proposed impact damage model. The results of both calculations were presented in the figures and compared with the test data.

Upon the loading path, the predictions based on the present model agreed with the data very well. The first load drop from the data corresponded quite well with the predicted load at which the initial damage was predicted due to matrix cracking and delamination. The calculations without considering the damage could not detect the load drop and overestimated the maximum load that the composite could sustain.

Upon unloading, both predictions with and without the inclusion of the damage model deviated from the data. As expected, the deviation can be attributed primarily to the Hertzian contact law, which was developed originally not for simulating the unloading response. However, by examining the predicted size of the accumulated damage, it was found that most of the damage in composites was generated along the loading path. Unloading could affect the post-impact dynamic response of the target, which is not of particular interest to the study.

Figure 11 shows the contact stiffness distribution of the impactor as a function of time during impact at three different velocities. Clearly, the contact stiffness

degraded once damage occurred in the laminate. At higher velocity at which damage accumulated faster, the rate of degradation was high. Upon unloading, the contact stiffness remained almost constant for all the cases studied.

Mass Effect

The effect of mass on the impact response of T800/3900-2 composites at a given impact energy was studied by Delfosse et al. [49]. Figures 12-15 showed the predicted force-time response as compared to the measurements taken from [49]. At the same impact energy, the impactor's mass affected significantly the force response. At a heavier mass, a single hump was found, but multiple humps were found for a lower mass. Again, the predictions matched with the data very well on the loading path. Upon unloading, the model predicted a longer duration of impact than was recorded in the experiments.

5.2 TOUGHENED V.S. UNTOUGHENED COMPOSITES

Numerical simulations were also generated to compare with the impact test data that were generated on composites with and without interleaves during the investigation. Figures 5-7 also show the comparison between the predictions and the measurements of the damage size as a function of impact energy. Clearly, the predictions agreed quite well with the measurements for the laminates with and without interleaves.

VI. COMPUTER CODE: 3DIMPACT

The computer code,"3DIMPACT," has been considerably modified based on the proposed model. The code has a user-friendly interactive mode for inputs. The code was developed for analyzing laminated composite plates subjected to transverse projectile impact. For a given mass and raduis of the impactor and the material

properties of a composite, the code is capable of producing the following results:

1) three-dimensional stress and strain distributions during the impact.

2) the impact force-time history.

3) the mode and the extent of the damage in every layer of the laminate due to impact.

4) the residual stiffness of the composite after impact.

A copy of the code can be obtained from Fu-Kuo Chang at the address given on the cover page.

VII. CONCLUSIONS

A model has been developed for predicting impact damage and residual properties of laminated composites. The model has been implemented in "3DIMPACT" code. Experiments were also conducted on laminates with and without toughening interleaves to verify the model and the computer simulations.

The predictions based on the model agreed with the measured force response upon loading very consistently. However, the predictions overestimated the duration of the impact upon unloading, which could be attributed to the Hertzian contact law. Meanwhile, the model predicted very well the impact damage size for materials with and without interleaves.

Based on the study the following remarks can be made:

(1) The force-time response of large-mass impact is more sensitive to impact damage than low-mass impact at the same impact energy.

(2) Alternating ply orientations produce smaller damage size than clustered ply orientations of the same thickness.

(3) Composites with toughened interfaces result in higher impact resistance.

(4) Interfacial shear strengths as well as transverse tensile strength are critical in governing impact damage size.

It is believed that the Hertzian contact law has to be further modified in order to study the unloading path during impact. A direct modelling of the impactor as an elastic or rigid body in the finite element simulation would be desired to avoid the uncertainty in the contact law.

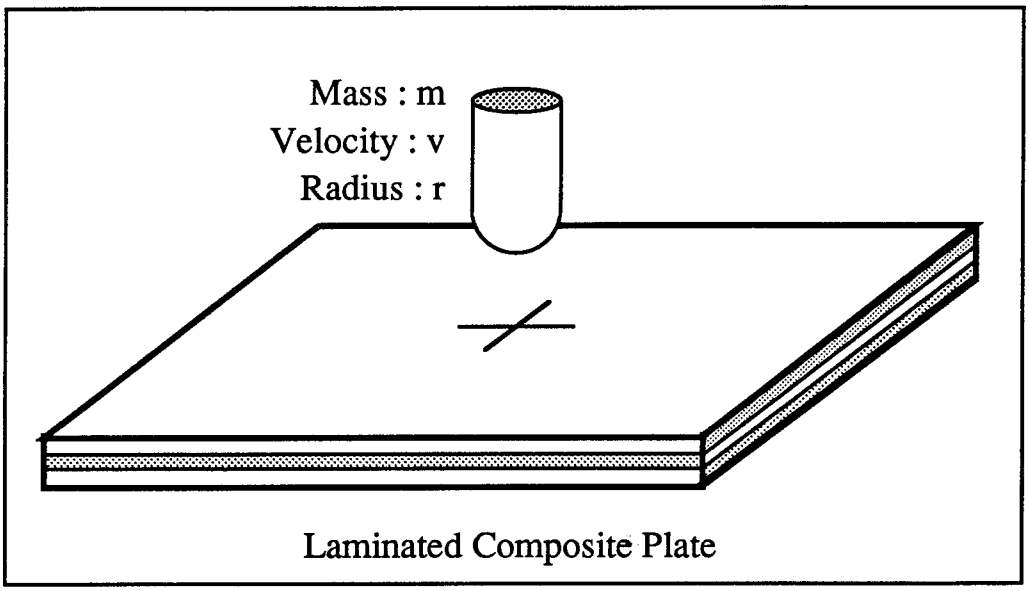

Figure 1 Description of the problem.

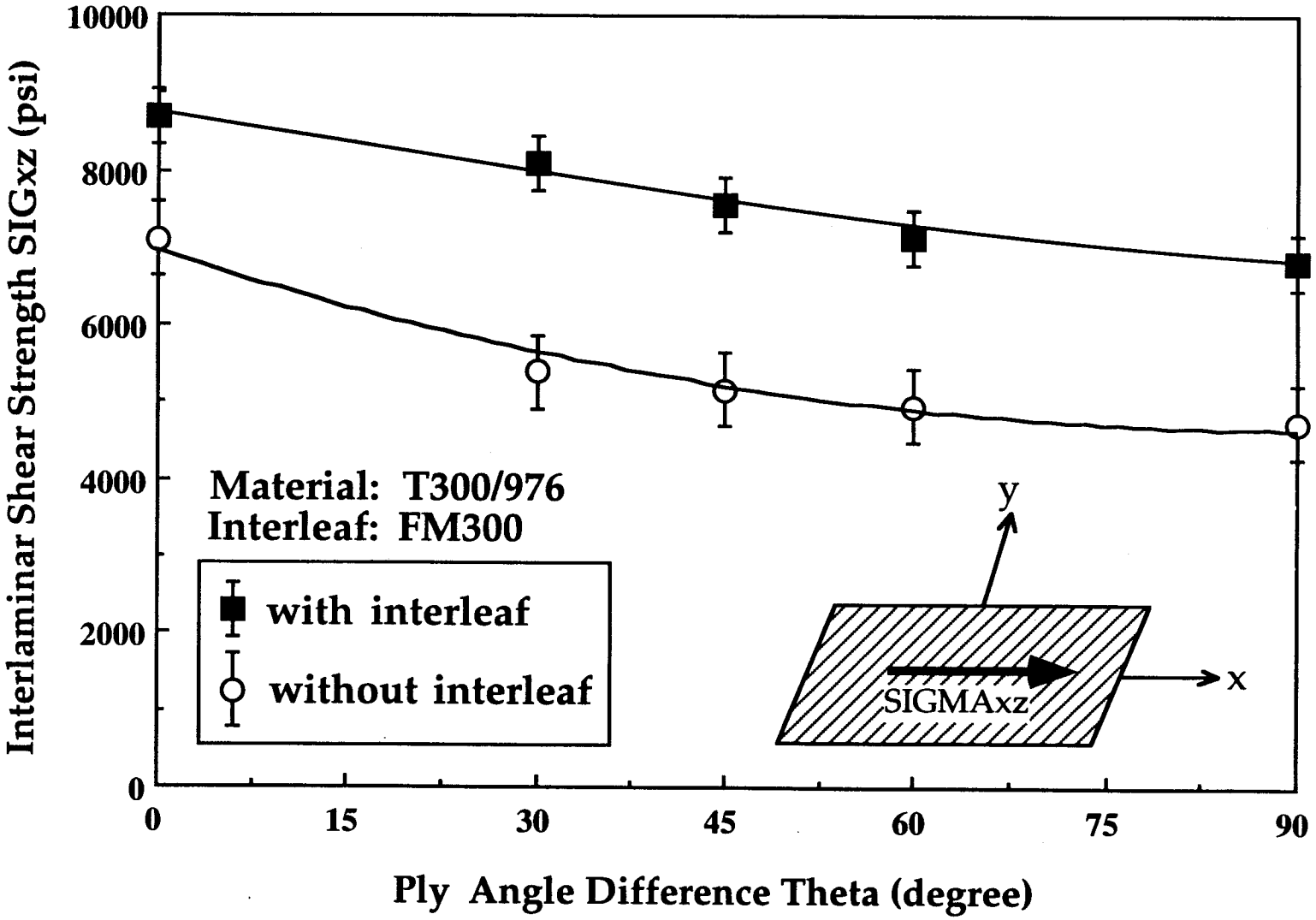

Figure 2 Interlaminar shear strength S_{xz} of a unidirectional ply in a laminate as a function of the ply angle mismatch with respect to its neighboring ply.

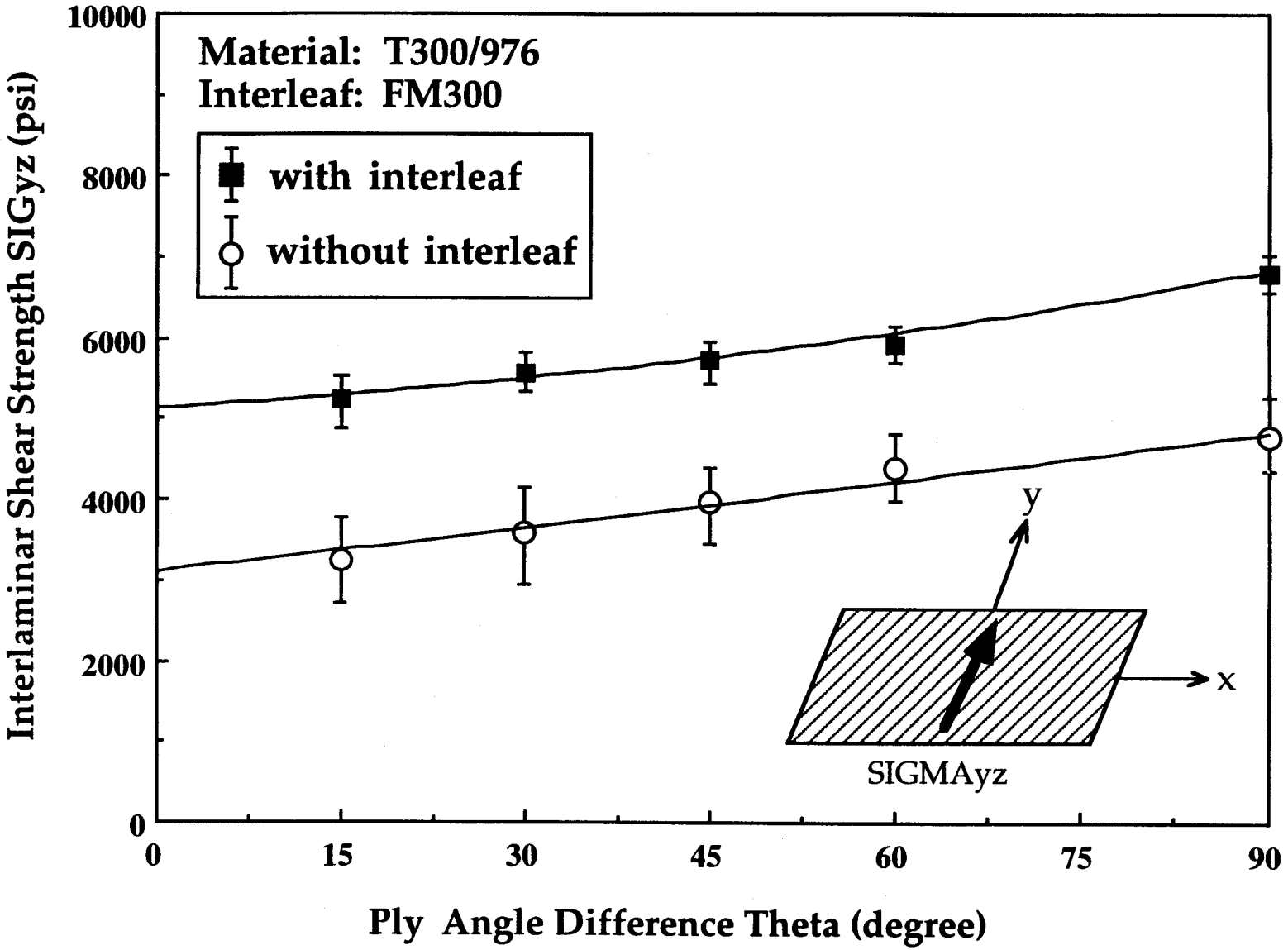

Figure 3 Interlaminar shear strength S_{yz} of a unidirectional ply in a laminate as a function of the ply angle mismatch with respect to its neighboring ply.

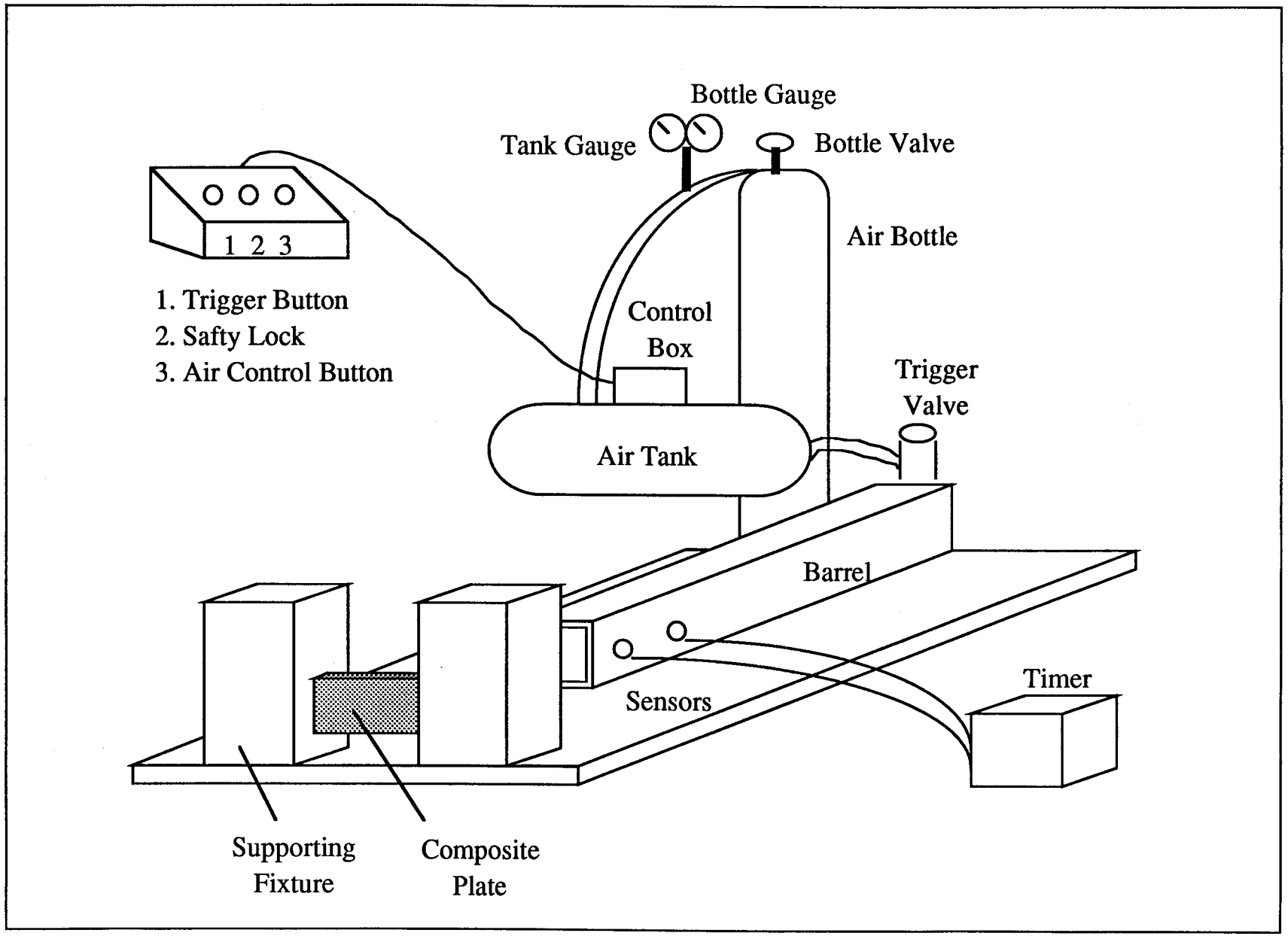

Figure 4 Schematic of the impact test set-up.

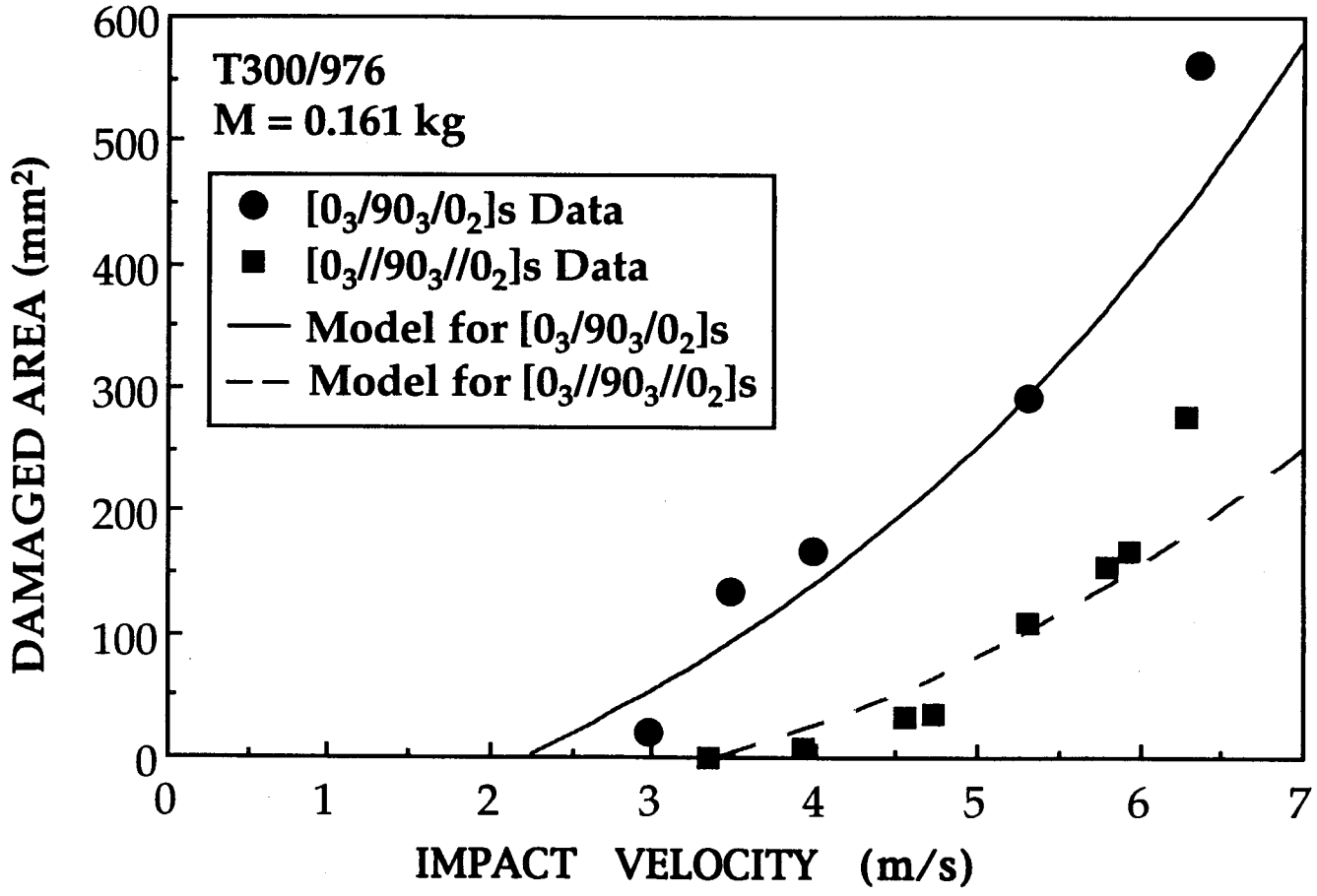

Figure 5 Impact damage area as a function of the impact velocity for composites with and without interleaves. Comparison between the predictions and the test data.

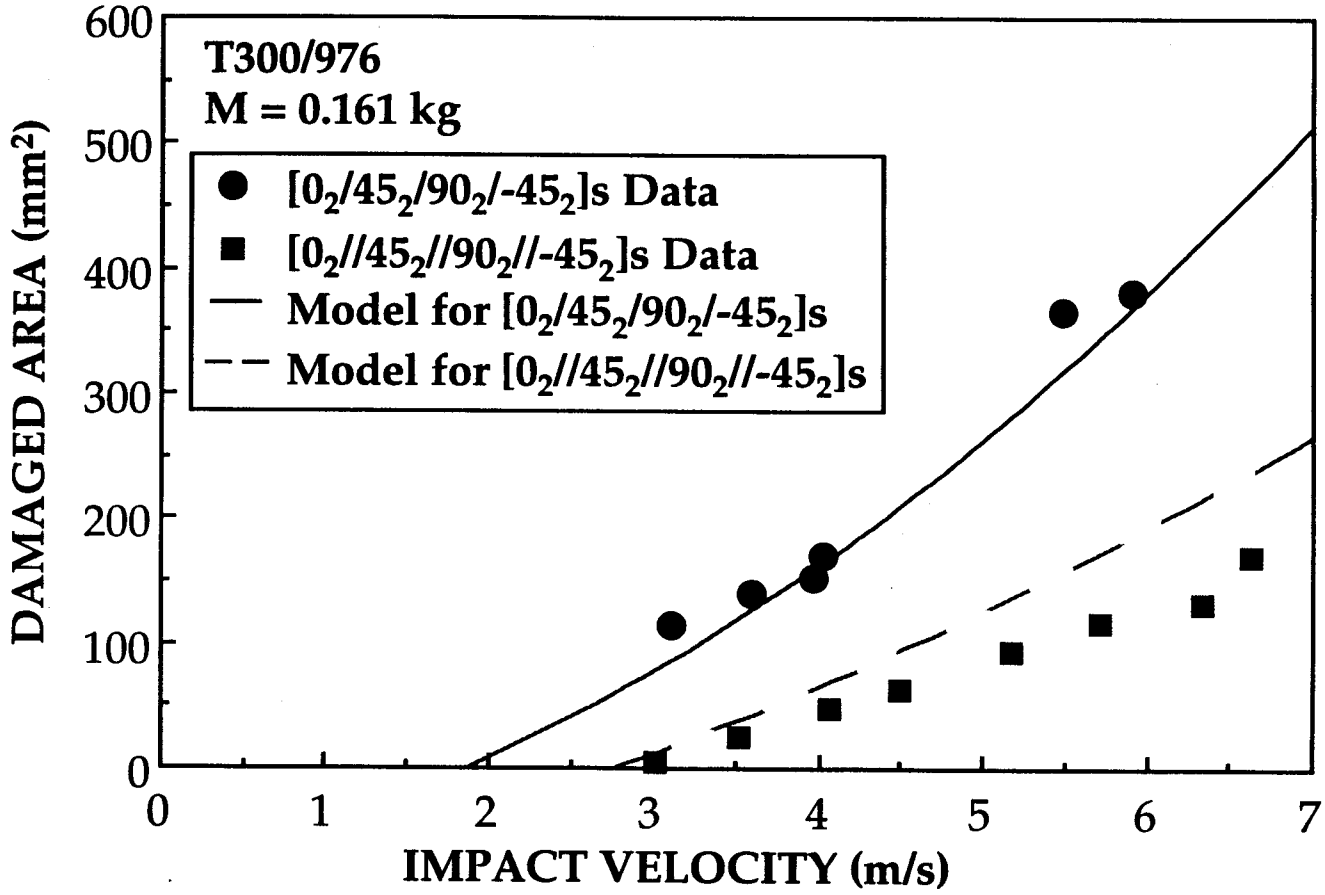

Figure 6 Impact damage area as a function of the impact velocity for composites with and without interleaves. Comparison between the predictions and the test data.

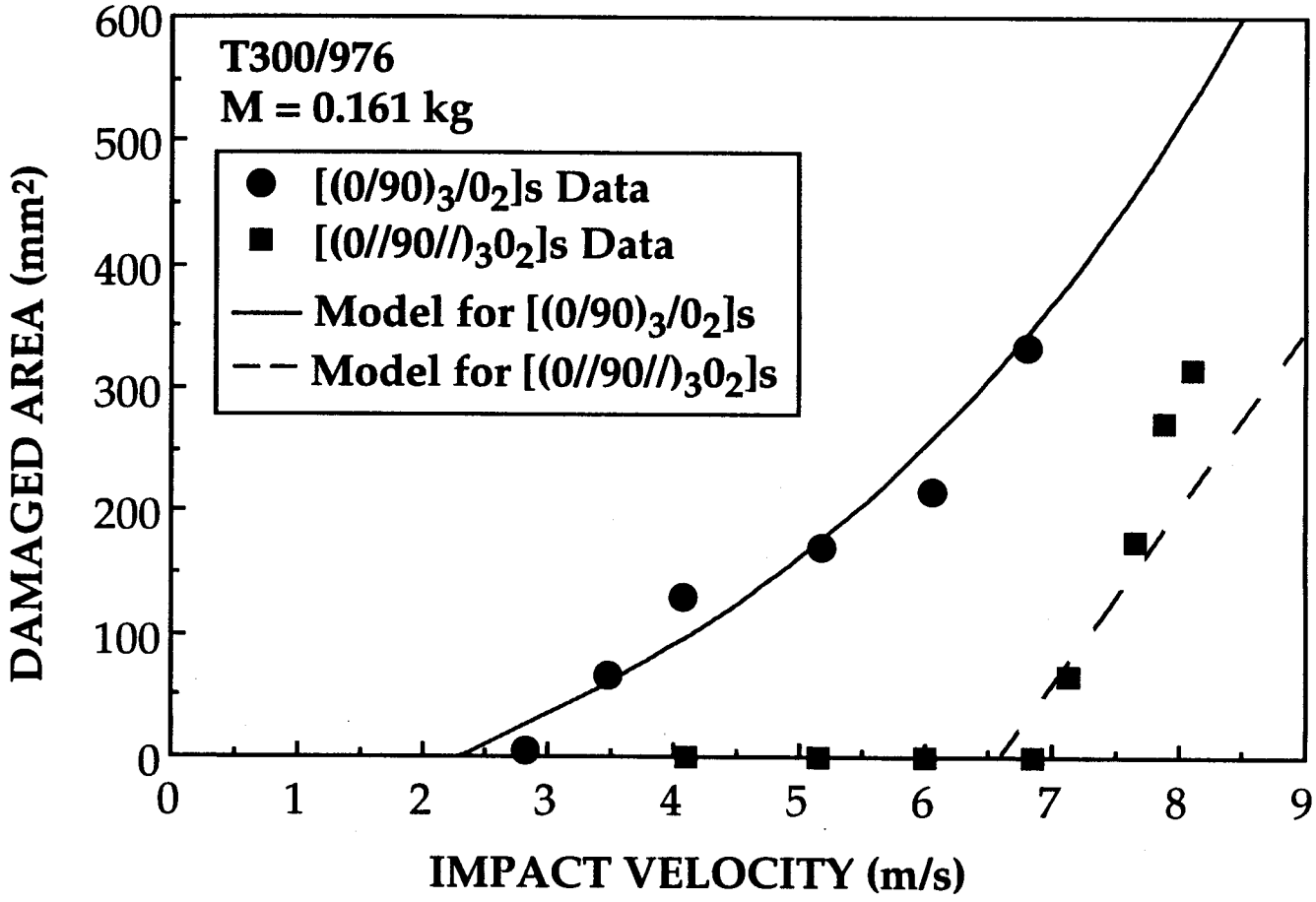

Figure 7 Impact damage area as a function of the impact velocity for composites with and without interleaves. Comparison between the predictions and the test data.

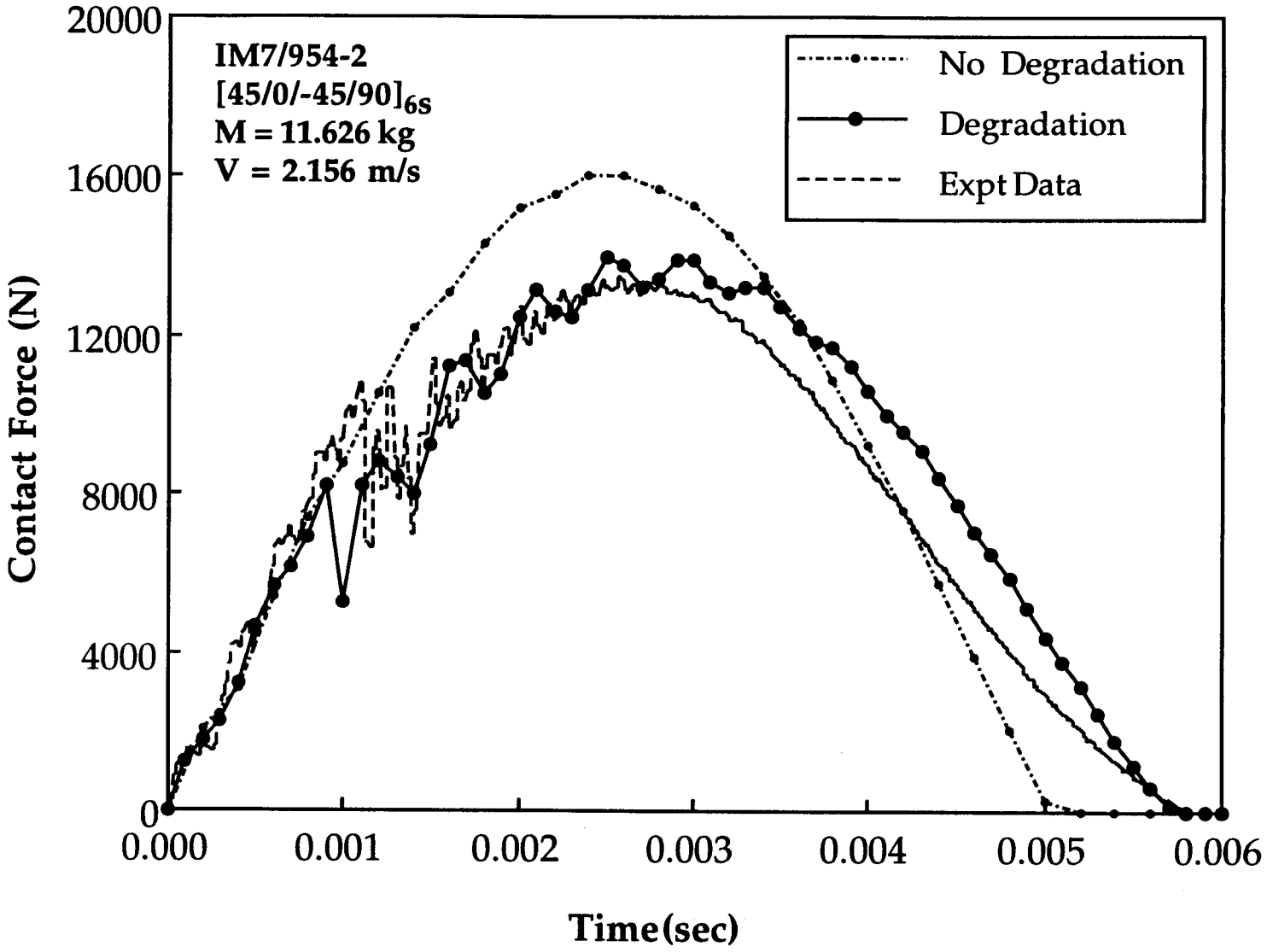

Figure 8 Impact force distribution as a function of time for IM7/954-2 graphite/epoxy composites. Comparison between the predictions with and without material degradation and the test data.

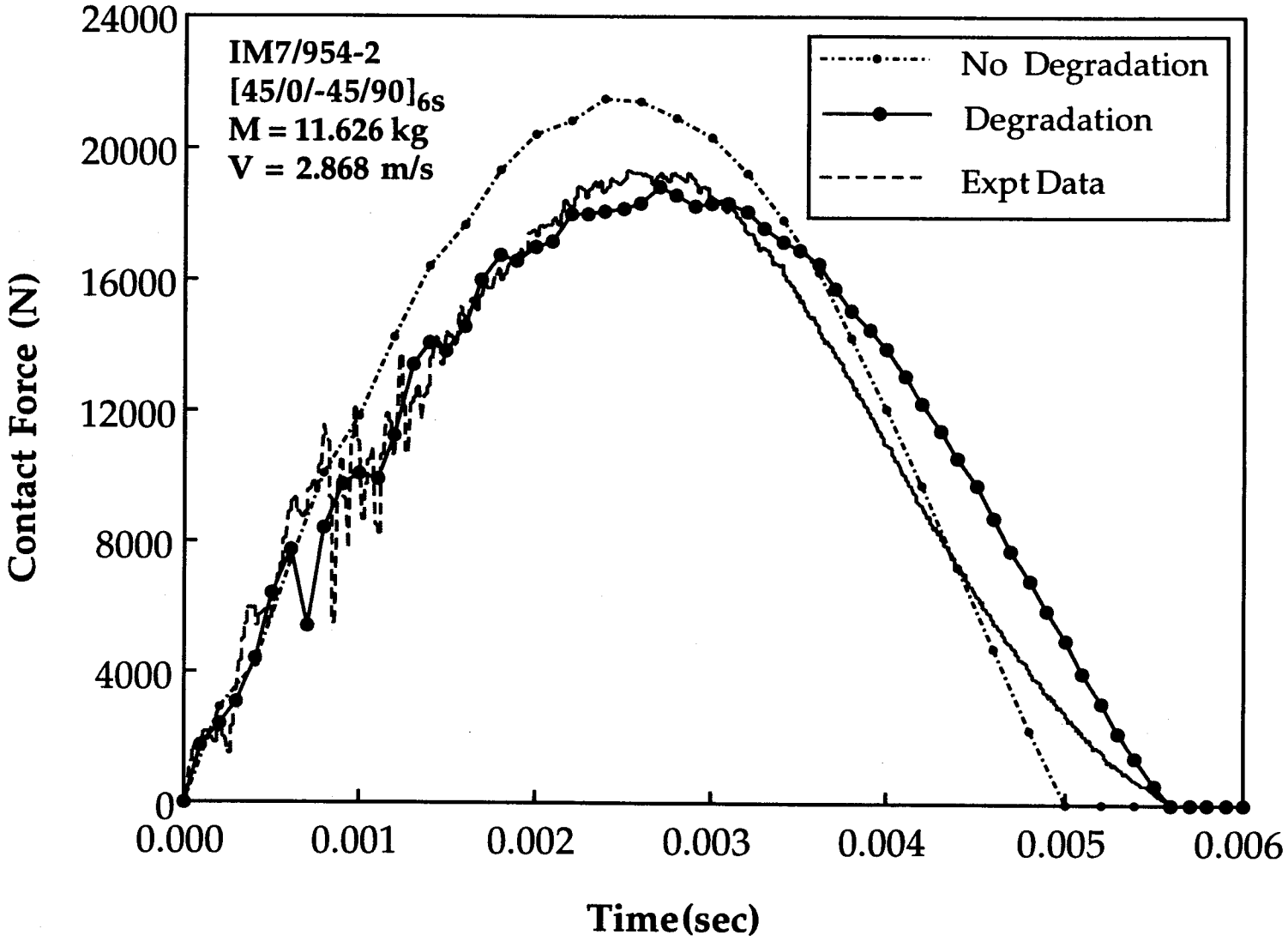

Figure 9 Impact force distribution as a function of time for IM7/954-2 graphite/epoxy composites. Comparison between the predictions with and without material degradation and the test data.

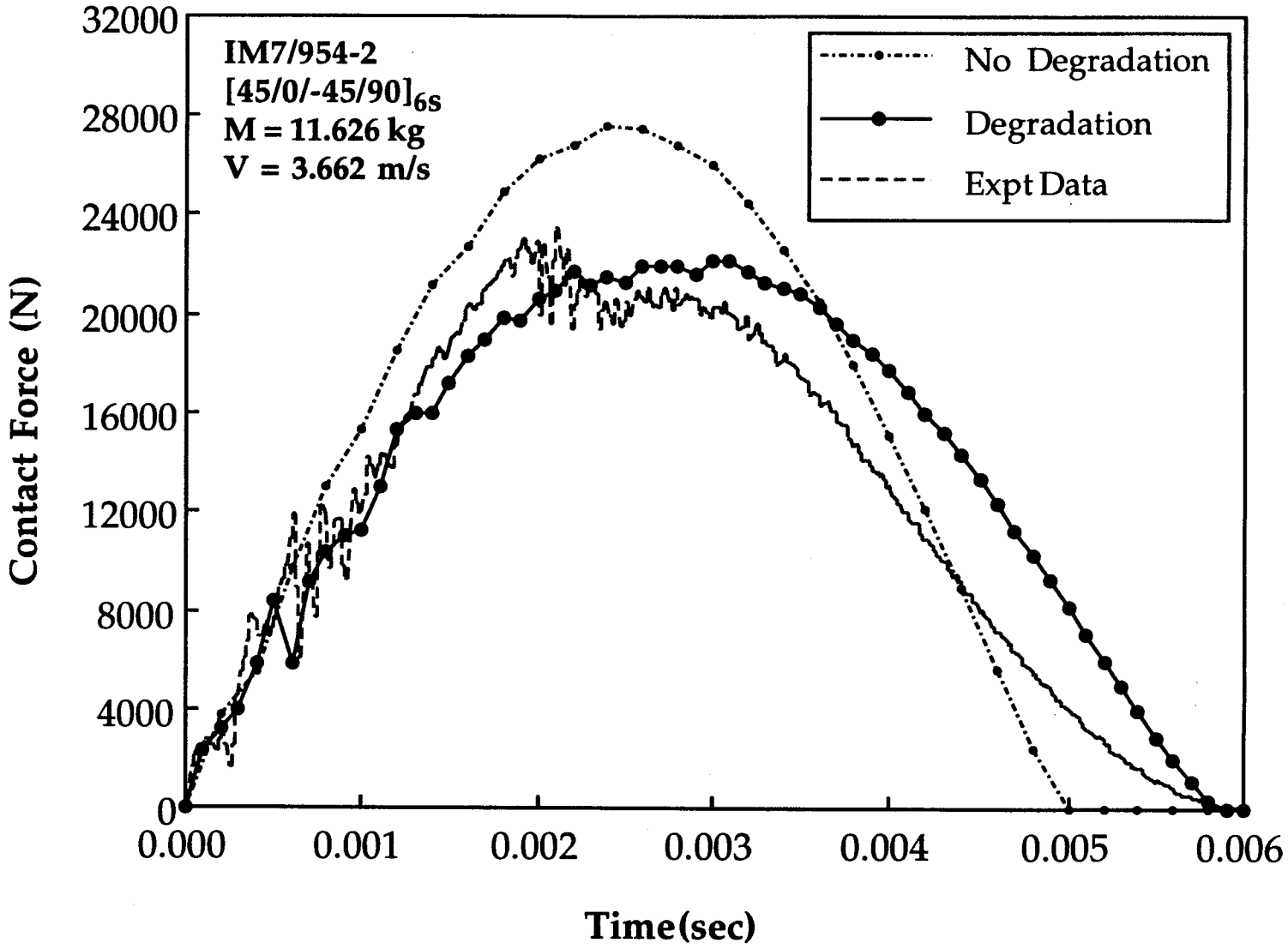

Figure 10 Impact force distribution as a function of time for IM7/954-2 graphite/epoxy composites. Comparison between the predictions with and without material degradation and the test data.

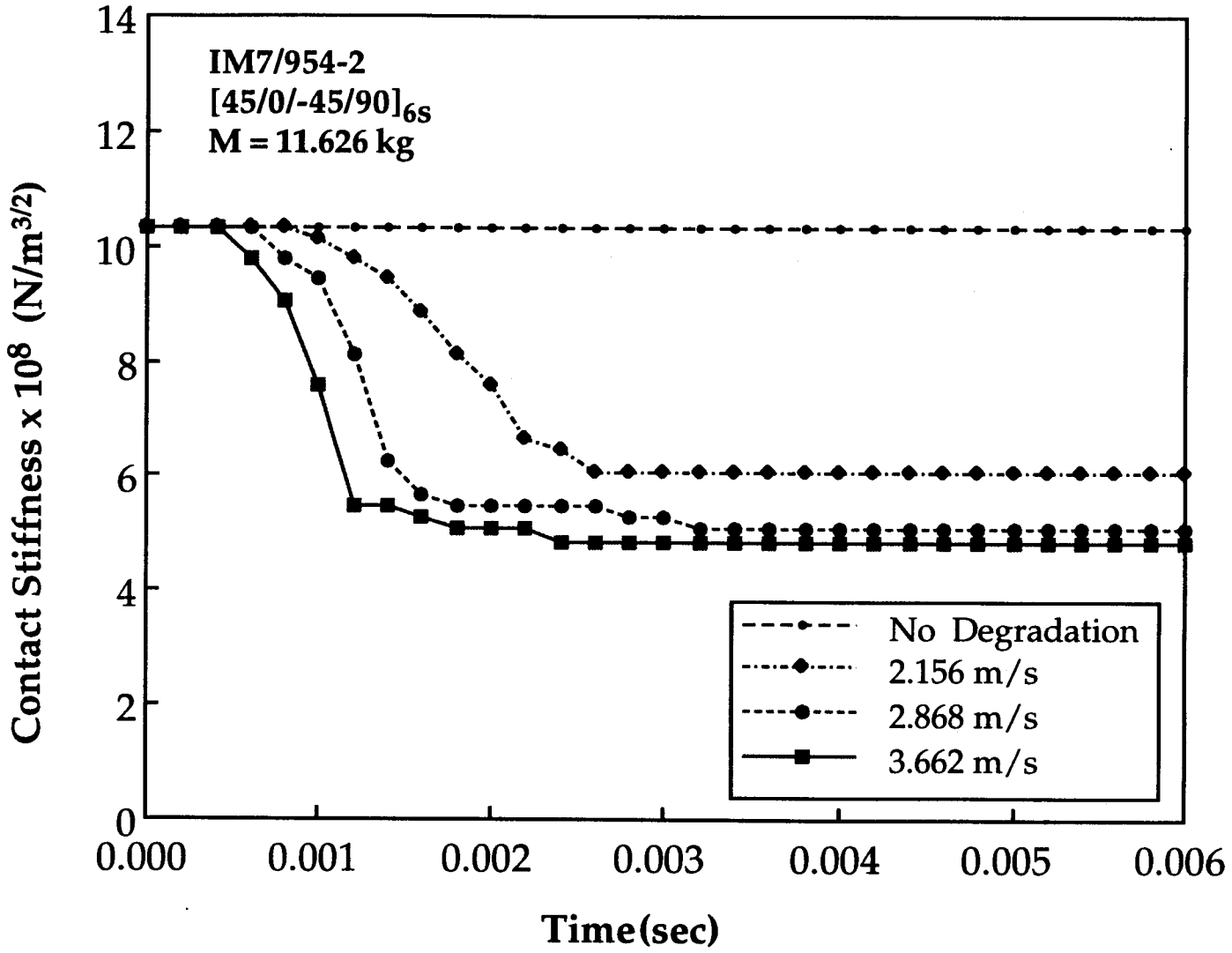

Figure 11 The distribution of the contact stiffness as a function of time during impact on IM7/954-2 graphite/epoxy composites for an impactors at three different velocities.

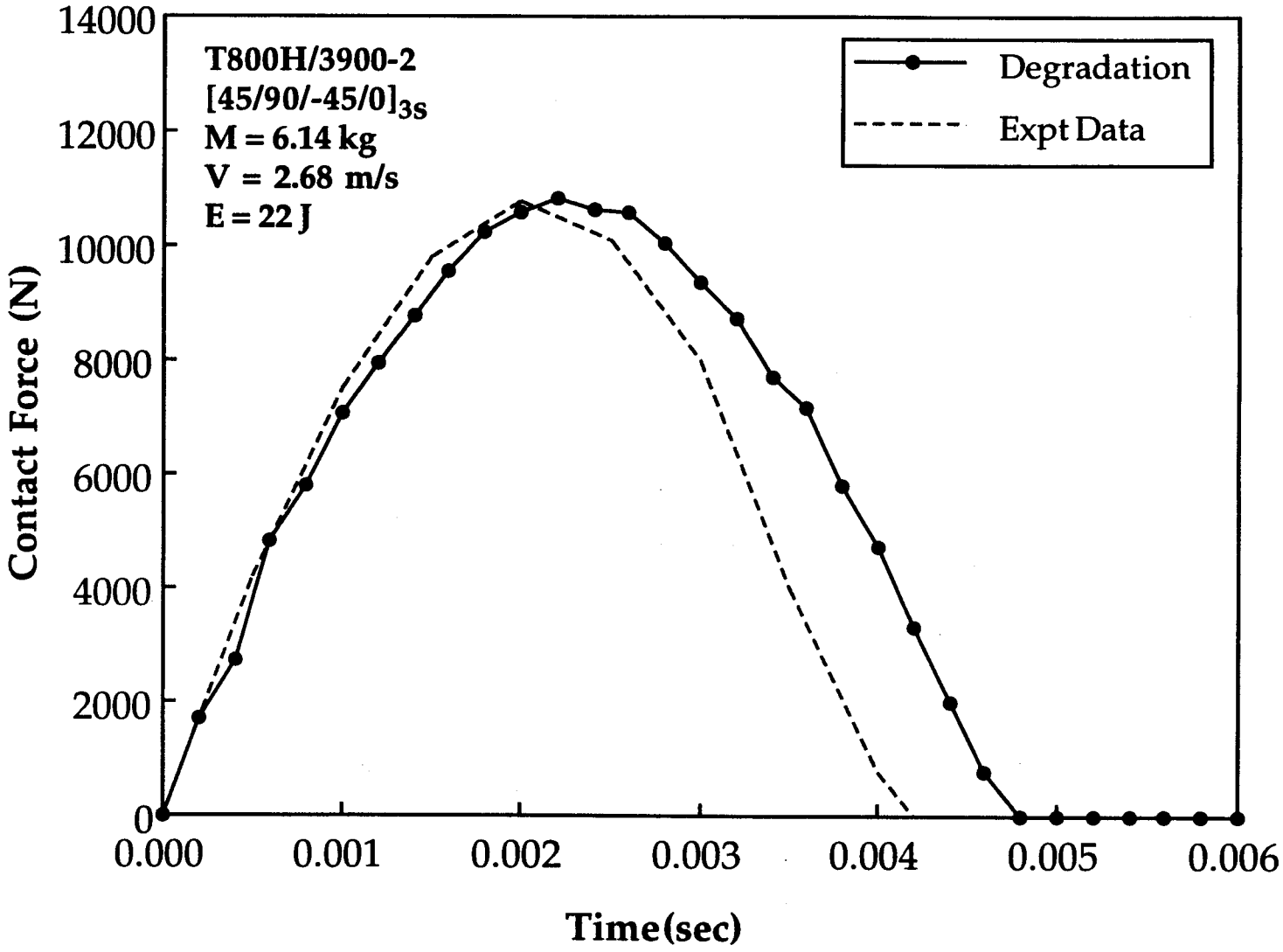

Figure 12 Impact force distribution as a function of time for T800/3900-2 graphite/epoxy composites. Comparison between the predictions based on the present model and the test data [49].

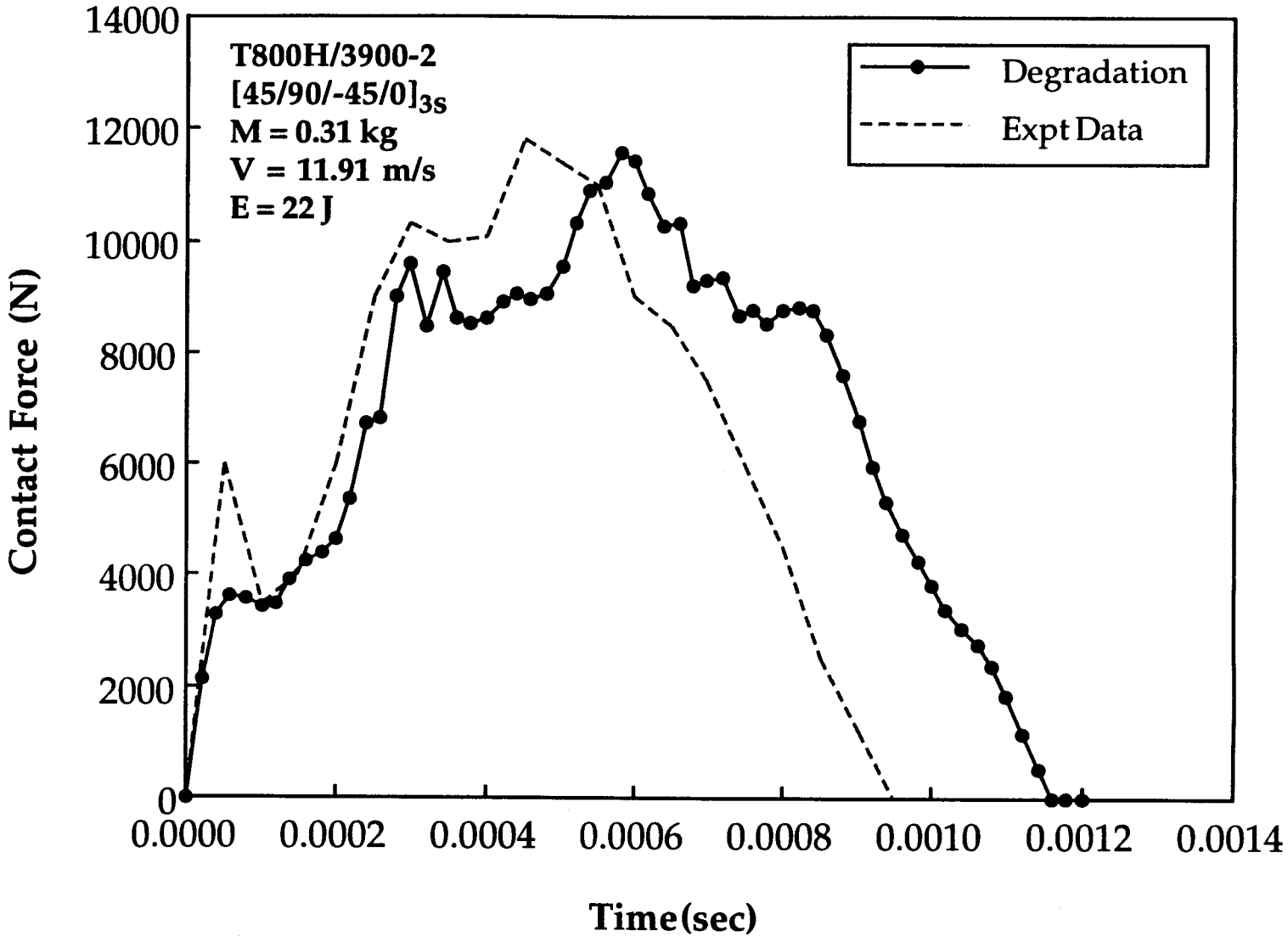

Figure 13 Impact force distribution as a function of time for T800/3900-2 graphite/epoxy composites. Comparison between the predictions based on the present model and the test data [49].

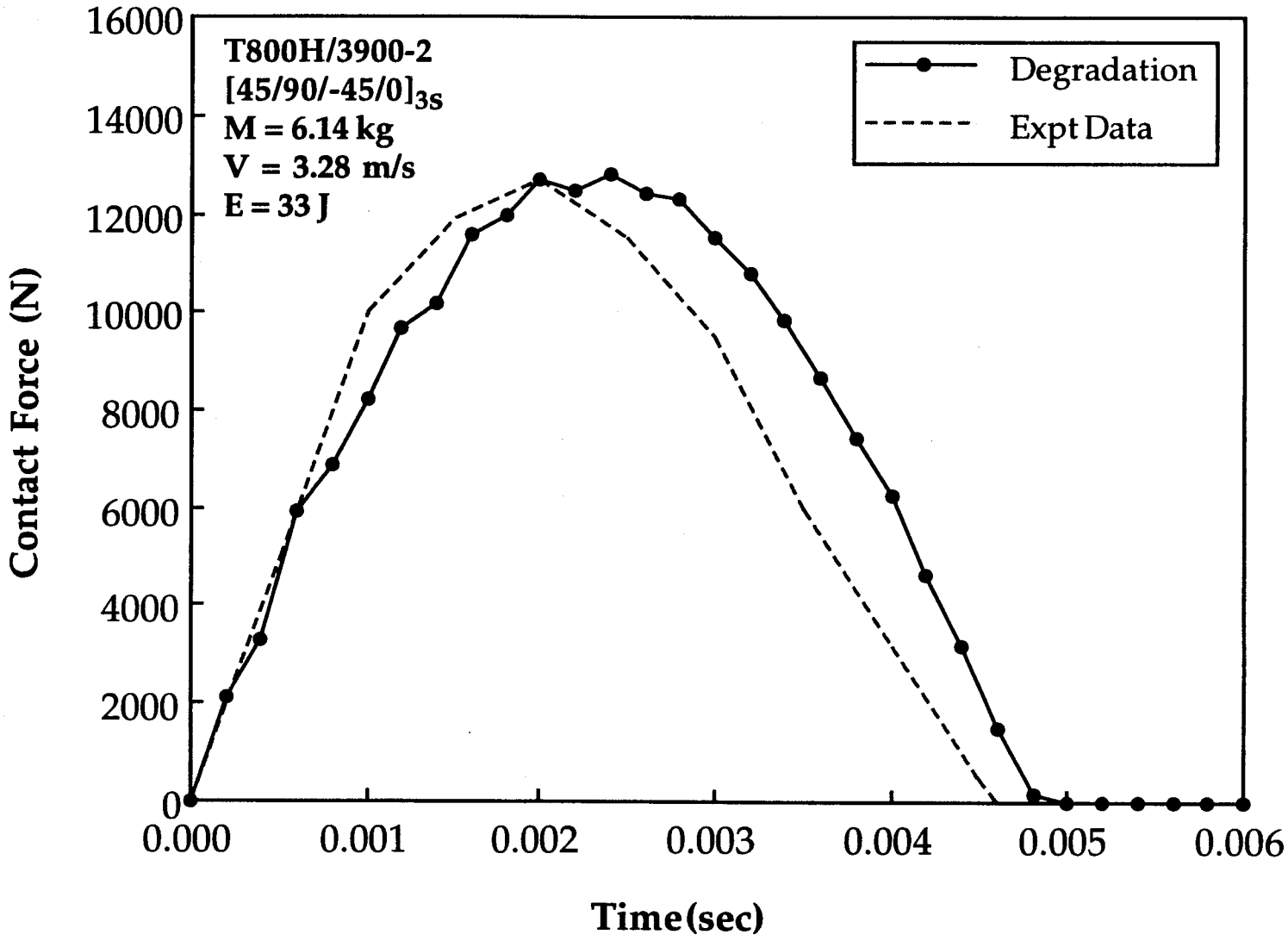

Figure 14 Impact force distribution as a function of time for T800/3900-2 graphite/epoxy composites. Comparison between the predictions based on the present model and the test data [49].

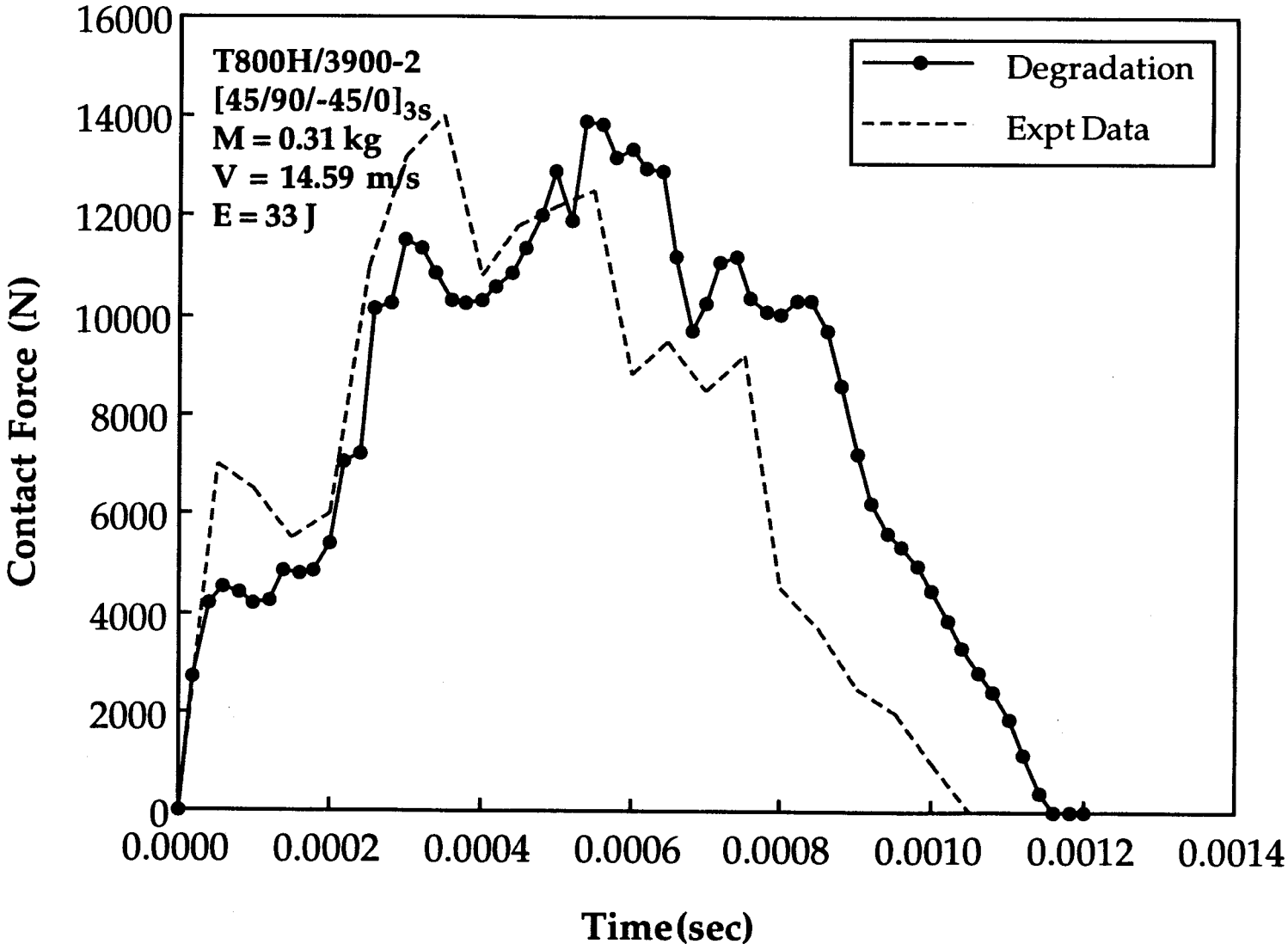

Figure 15 Impact force distribution as a function of time for T800/3900-2 graphite/epoxy composites. Comparison between the predictions based on the present model and the test data [49].

VIII. REFERENCES

[1]. Guynn, E. G. and O'Brien, T. K., "The Influence of Lay-up and Thickness on Composite Impact Damage and Compression Strength," Proceedings of AIAA /ASME/ASCE/AHS, 26th SDM Conference, Orlando, FL (1985), pp. 187–196.

[2]. Choi, H. Y., Downs, R. J. and Chang, F. K., "A New Approach Toward Understanding Damage Mechanisms and Mechanics of Laminated Composites Due to Low-Velocity Impact, Part I–Experiments," J. of Composite Materials, Vol. 25 (1991), pp. 992-1011.

[3]. Choi, H. Y., Wu, H. Y. T. and Chang, F. K., "A New Approach Toward Understanding Damage Mechanisms and Mechanics of Laminated Composites Due to Low-Velocity Impact, Part II–Analysis," J. Composite Materials, Vol. 25 (1991), pp. 1012-1038.

[4]. Choi, H. Y., Wang, H. S. and Chang, F. K., "Effect of Laminate Configuration and Impactor's Mass on the Initial Impact Damage of Composite Plates Due to Line-Loading Impact," J. of Composite Materials, Vol. 26, No. 6 (1992), pp. 804-427.

[5]. "Composite Plates Impact Damage - An Atlas," by S. Finn and G.S. Springer, Technomic Publishing, 1991.

[6]. Masters, J.E., "Structural Performance and Impact Resistance of Advanced Interleaved Materials," *Proceedings of 34th International SAMPE Symposium* (1989), pp. 1792-1802.

[7]. Odagiri, N., Kishi, H. and Nakae, T., "T800H/3900-2 Toughened Epoxy Prepreg System: Toughening Concepts and Mechanisms," *Proceedings of 34th International SAMPE Symposium* (1989), pp. 43-52.

[8]. Elber, W., "Failure Mechanics in Low-Velocity Impacts on Thin Composite Plates," NASA Technical Paper TP 2152, NASA-Langley Research Center, Hampton, VA (1983).

[9]. Joshi, S. P. and Sun, C. T., "Impact-Induced Fracture in Quasi-Isotropic Lami-

nate," J. Composite Technology and Research, Vol. 19 (1986), pp. 40–46.

[10]. Cantwell, W. J. and Morton, J., "Geometrical Effects in the Low Velocity Impact Response of CFRP," Composite Structures, Vol. 12 (1989), pp. 39–59.

[11]. Sjoblom, P. O., Hartness, J. T. and Cordell, T. M., "On Low-Velocity Impact Testing of Composite Materials," J. Computers and Structures, Vol. 22 (1988), pp. 30–52.

[12]. Greszczuk, L. B., "Foreign Objects Damage to Composites," ASTM STP 568 (1973).

[13]. Chamis, C. C. and Sinclair, J. H., "Impact Resistance of Fiber Composites: Energy-Absorbing Mechanisms and Environmental Effects," Recent Advances in Composites in the United States and Japan, ASTM STP 864 (Vinson and Taya, Eds.) (1983), pp. 326–345.

[14]. Chamis, C. C., Hanson, M. P. and Serafini, T. T., "Designing for Impact Resistance with Unidirectional Fiber Composites," NASA TND-6463, National Aeronautical and Space Administration, Washington, D.C. (1971).

[15]. Wu, H. T. and Springer, G. S., "Measurements of Matrix Cracking and Delamination Caused by Impact on Composite Plates," J. of Composite Materials, Vol. 22 (1988), pp. 518–532.

[16]. Wu, H. T. and Springer, G. S., "Impact Induced Stresses, Strains and Delaminations in Composite Plates," J. of Composite Materials, Vol. 22 (1988), pp. 533–560.

[17]. Gosse, J. H. and Mori, P. B. Y., "Impact Damage Characterization of Graphite/ Epoxy Laminates," Proceedings of the Third Technical Conference of the American Society for Composites, Seattle, WA (1988), pp. 334–353.

[18]. Joshi, S. P., "Impact-Induced Damage Initiation Analysis: An Experimental Study," *Proceedings of the Third Technical Conference of the American Society for Composites*, Seattle, WA (1988), pp. 325–333.

[19]. Sun, C. T. and Rechak, S., "Effect of Adhesive Layers on Impact Damage

in Composite Laminates," Composite Materials: Testing and Design (Eighth Conf.), ASTM STP 972 (J. D. Whitcomb, Ed.), American Society for Testing and Materials, Philadelphia, PA (1988), pp. 97–123.

[20]. Clark, G., "Modelling of Impact Damage in Composite Laminate," Composites, Vol. 20 (1988), pp. 209–214.

[21]. Reed, P. E. and Turner, S., "Flexed Plate Impact, Part 7. Low Energy and Excess Energy Impacts on Carbon Fiber-Reinforced Polymer Composites," Composites, Vol. 19 (1988), pp. 193–203.

[22]. Liu, D. and Malvern, L. E., "Matrix Cracking in Impacted Glass/Epoxy Plates," J. Computers and Structures, Vol. 21 (1987), pp. 594–609.

[23]. Gu, Z. L. and Sun, C. T., "Prediction of Impact Damage Region in SMC Composites," Composite Structures, Vol. 7 (1987), pp. 179–190.

[24]. Chen, J. K. and Sun, C. T., "'Analysis of Impact Response of Buckled Composite Laminates," Composite Structures, Vol. 3 (1985), pp. 97–118.

[25]. Chen, J. K. and Sun, C. T., "On the Impact of Initially Stressed Composite Laminates," J. of Composite Materials, Vol. 19, Nov. (1985), pp. 490–504.

[26]. Stori, A. A. and Magnus, E., "An Evaluation of the Impact Properties of Carbon Fiber Reinforced Composites with Various Matrix Materials," J. of Composite Structures, Vol. 2 (1983), pp. 332–248.

[27]. Malvern, L. E., Sierakowski, R. L., Ross, L. A. and Cristescu, N., "Impact Failure Mechanisms in Fiber-Reinforced Composite Plates," High Velocity Deformation of Solids (Kawata and Shiori, Eds.), Springer-Verlag, Berlin (1978), pp. 120–130.

[28]. Jones, S., Paul, J., Tay, T. E. and Williams, J. F., "Assessment of the Effect of Impact Damage in Composites: Some Problems and Answers," Composite Structures, Vol. 10 (1988), pp. 51–73.

[29]. Poe, Jr., C. C., "Simulated Impact Damage in a Thick Graphite /Epoxy Laminate using Spherical Indenters," NASA TM–100539, January (1988).

[30]. Finn, S. and Springer, G. S., "Delaminations in Composite Plates Under Transverse Static or Impact Loads—A Model," J. of Composite Structures, Vol. 23 (1993), pp. 177–190.

[31]. *NASA Workshop on Impact Damage to Composites*, compiled by C.C. Poe, Jr., NASA Conference Publication 10075, July, 1991.

[32]. Sun, C. T. and Yang, S. H., "Contact Law and Impact Responses of Laminated Composites," NASA CR-159884, National Aeronautical and Space Administration, Washington, D.C. (1980).

[33]. Tan, T. M. and Sun, C. T., "Use of Statical Indentation Laws in the Impact Analysis of Laminated Composite Plates," J. of Applied Mechanics, Vol. 52, (1985), pp. 6–12.

[34]. Kubo, J. T. and Nelson, R. B., "Analysis of Impact Stresses in Composite Plates," American Society for Testing and Materials, Special Technical Publication 568, Philadelphia, PA (1975), pp. 228–244.

[35]. Wu, H. T. and Chang, F. K., "Transient Dynamic Analysis of Laminated Composite Plates Subjected to Transverse Impact," J. of Computers and Structures, Vol. 31 (1989), pp. 453–466.

[36]. Ross, C. A. and Malvern, L. E., Sierakowski, R. L. and Taketa, N., "Finite-Element Analysis of Interlaminar Shear Stress Due to Local Impact," Recent Advances in Comp. in the United States and Japan, ASTM STP 864 (J. P. Vinson and M. Taya, Eds.), American Society for Testing and Materials, Philadelphia, PA (1985), pp. 335–367.

[37]. Aggour, H. and Sun, C. T., "Finite Element Analysis of a Laminated Composite Plate Subjected to Circularly Distributed Central Impact Loading," J. Computers and Structures, Vol. 28 (1988), pp. 729–736.

[38]. Kim, B. S. and Moon, F. C., "Transient Wave Propagation in Composite Plates Due to Impact," *Proceedings of the AIAA/ASME 18th Structures, Structural Dynamics and Materials Conference,* Vol. B, San Diego, CA, March 1977, pp.

43–50.

[39]. Ross, C. A., Malvern, L. E., Sierakowski, R. L. and Taketa, N., "Finite-Element Analysis of Interlaminar Shear Stress Due to Local Impact," Recent Advances in Composites in the United States and Japan, ASTM STP 864 (Vinson and Taya, Eds.) (1983), pp. 355–367.

[40]. Lal, K. M., "Low Velocity Transverse Impact Behavior of 8-ply Graphite-Epoxy Laminates," J. of Reinforced Plastics and Composites, Vol. 2 (1983), pp. 216–225.

[41]. Sun, C. T. and Chattopadhyay, S., "Dynamic Response of Anisotropic Laminated Plates Under Initial Stress to Impact of a Mass," J. of Applied Mechanics, Vol. 42 (1975), pp. 693–698.

[42]. Choi, H. Y. and Chang, F. K., "A Model For Predicting Impact Damage of Graphite/Epoxy Laminated Composites Due to Point-Nose Impact," J. of Composite Materials, Vol. 26, No. 14, (1992), pp. 2134–2169.

[43]. Lee, S. G. and Chang, F. K., "Impact Damage Resistance of Laminated Composites with Toughened Interfaces," *Proceedings of ICCM/9 (International Conference on Composite Materials),* Vol. V, Madrid, Spain, 1993, pp. 307–310.

[44]. Lee, S., "Impact Damage Tolerance of Composites," Ph.D. dissertation of Department of Aeronautics and Astronautics, Stanford University (1994).

[45]. Shahid, I. and Chang, F. K., "An Accumulative Damage Model for Tensile and Shear Failures of Laminated Composite Plates," *J. of Composite Materials* (to appear, 1994).

[46]. Hertz, O., "Ueber die Berührung fester elastischer Körper," J. für die Reine und Angewandte Mathematik, 92 (1982), pp. 156–171.

[47]. Greszczuk, L. B. and Chao, H., "Impact Damage in Graphite-Fiber-Reinforced Composites," *Composite Materials: Testing and Design (Fourth Conference), ASTM STP 617,* American Society for Testing and Materials (1977), pp. 389-408.

[48]. Cairns, D.S. and Lagace, P. A., "Thick Composite Plates Subjected to Lateral Loading," *J. of Applied Mechanics, Vol. 54* (1987), pp. 611-616.

[49]. Delfosse, D., Poursartip, A., Coxon, B. R., and Dost, E. F., "Non-Penetrating Impact Damage of CFRP at Low and Intermediate Velocities," *Proceedings of the Fifth Symposium of Composite Materials: Fatigue and Fracture,* American Society of Testing and Materials (ASTM) (1993), Atlanta, GA.

[50]. Shahid, I., S. K. Lee, and Chang, F. K., "Impact Damage Tolerance of Textile Composites," Final report to Lockheed Aeronautical Systems Company, Marietta, GA, 1994.